Formation of Liquid Crystals from Actin Filaments†

Ruth Furukawa, Robin Kundra,‡ and Marcus Fechheimer*

Department of Zoology, University of Georgia, Athens, Georgia 30602

Received March 24, 1993; Revised Manuscript Received September 16, 1993®

ABSTRACT: Actin is cross-linked by actin-binding proteins in the cytoplasm to form either isotropic or highly oriented anisotropic structures. The inherent orientation among actin filaments could influence whether an isotropic or highly oriented anisotropic structure is formed. A highly oriented state can arise spontaneously through the formation of liquid crystals as predicted by polymer theory. In this study, the ability of filamentous actin to form liquid crystalline domains was detected using the anisotropic component of scattered light and by observation of birefringence. As liquid crystalline domains formed, the intensity of the anisotropic component of scattered light increased, and birefringent macroscopic oriented domains were directly observed. The formation of liquid crystalline domains was dependent on the concentration of actin filaments and on the average filament length controlled by varying the ratio of gelsolin to actin monomers. The concentration of actin filaments required to form liquid crystalline domains increased moderately as the average length was decreased. At a fixed actin concentration, orientation among the filaments attained a maximum value at a ratio of actin to gelsolin in the range from 1500 to 2000 and decreased as the ratio was increased or decreased from this range. The results are not well explained by theoretical treatments for liquid crystal formation by monodisperse, charged worm-like chains. Differences from the theoretical predictions for formation of liquid crystals are most likely due to the polydisperse filament length of actin. This phenomenon may have important effects on the structural and rheological properties of the cytoplasm in living cells.

Cell shape and movement are influenced by the mechanical properties and organization of the macromolecular components of cytoplasm. These structures are composed primarily of actin filaments, microtubules, and their associated proteins. The number, length, polarity, and orientation of fibrillar structures present at a given time may be approximated as a minimum (or local minimum) in the free energy state of this diverse mixture of components. Studies of the physical chemical behavior of purified actin and tubulin have therefore been the focus of intensive investigations by scientists seeking to understand the complex and dynamic changes in cytoplasmic structures accompanying cell movements. The focus of the present investigation is the formation of spontaneously aligned liquid crystalline domains in solutions of actin filaments. The alignment and polarity of filaments has significance for the biological and structural properties of these polymeric macromolecules.

Both actin filaments and microtubules are highly elongated and are relatively stiff molecules. These two attributes give rise to physical properties which have been theoretically modeled by polymer chemists. One property is that of liquid crystal formation—a phase transition involving formation of domains of polymer molecules with a high degree of intermolecular orientation. Microtubules are quite rigid, and their behavior is well approximated as rigid rod-like cylindrical molecules. Actin filaments are relatively stiff molecules with a persistence length that has been reported to be from 6 to 17.7 μm (Burlacu et al., 1992; Gittes et al., 1993; Nagashima & Asakura, 1980; Oosawa, 1980; Yanagida et al., 1984) and can be modeled as worm-like chains. Theories that relate the polymer concentration required for formation of the liquid crystal phase to the length and diameter of either stiff rod-like molecules or worm-like chains have been developed on the basis of the initial assumption that two molecules cannot occupy the same space (Odijk, 1986; Onsager, 1949). These theories are useful for analysis of the observed behavior of actin with respect to the physical models.

Nematic liquid crystal formation has been analyzed for both actin (Buxbaum et al., 1987; Coppin & Leavis, 1992; Kerst et al., 1990; Suzuki et al., 1991) and microtubules (Hitt et al., 1990). The studies of actin filaments employed rheological methods (Buxbaum et al., 1987; Kerst et al., 1990), anisotropic absorbance (Suzuki et al., 1991), and birefringence and polarization of fluorescence (Coppin & Leavis, 1992). However, three of the previous investigations intentionally introduced shear forces either during formation of the liquid crystals or during their measurement. In addition, all of the previous investigations utilized actin containing capping protein and/or variable numbers of aggregates and endogenous nuclei not removed by gel filtration, resulting in an uncontrolled filament length and number. These results emphasize the need to study spontaneous alignment under conditions in which application of exogenous shear forces is minimized.

In this study, the ability of filamentous actin to form liquid crystalline solutions was reinvestigated. The ability of actin filaments to form liquid crystalline domains with minimal levels of shear forces in the solutions was studied as a function of filament length and actin concentration using freshly column purified actin throughout. The results reveal formation of liquid crystal domains at actin concentrations significantly lower than previously demonstrated and allow comparison of the results to theoretical models of liquid crystal formation. The results have important implications for the formation of oriented structures of actin filaments in cytoplasm, and for

† This work was supported by a grant from the National Science Foundation (DCB-9105087) to M.F.

* Address correspondence to this author.

‡ Present address: Washington University School of Medicine, St. Louis, MO.

® Abstract published in *Advance ACS Abstracts*, November 1, 1993.

0006-2960/93/0432-12346$04.00/0

studies of actin dynamics and rheology *in vitro*. A preliminary report of this work was presented at the Annual Meeting of the American Society for Cell Biology (Furukawa et al., 1992).

MATERIALS AND METHODS

Purification of Rabbit Skeletal Muscle Actin. Actin was purified from an acetone powder of rabbit skeletal muscle essentially as described by Spudich and Watt (1971) with two cycles of assembly and sedimentation through 0.8 M KCl and then fractionated on a 2.5 × 64 cm column of Sephadex G-150 in 2 mM Tris, 0.2 mM ATP, 0.2 mM $CaCl_2$, 0.2 mM dithiothreitol, and 0.02% sodium azide, pH 8.0 (MacLean-Fletcher & Pollard, 1980). Actin was held in dialysis for at most 4 days with buffer changes every 24 h. The concentration range of actin studied is limited to the concentration directly eluted from the G-150 column. Further concentration of actin was not performed to minimize endogenous sources of nucleation other than that induced by gelsolin and to ensure that all actin present was capable of polymerization. The concentration of monomeric rabbit skeletal muscle actin was determined using an extinction coefficient of 0.62 mg^{-1} mL cm^{-1} at 290 nm.

Purification of Gelsolin. Gelsolin was purified essentially as described previously (Cooper et al., 1987). Bovine serum was dialyzed for 24 h versus 25 mM Tris, 0.5 mM $CaCl_2$, and 0.2 mM phenylmethanesulfonyl fluoride, pH 7.5. The serum was clarified in a GSA rotor for 15 min at 5000 rpm and applied to a DE-52 column (13 × 10 cm) previously equilibrated in 25 mM Tris, 0.5 mM $CaCl_2$, and 0.2 mM phenylmethanesulfonyl fluoride, pH 7.5. EGTA was added to the unbound fraction to a final concentration of 5 mM, and the pH was adjusted to pH 7.5. The sample was applied to a DE-52 column (20 × 2.5 cm) previously equilibrated with 25 mM Tris and 0.1 mM EGTA, pH 7.5 (buffer A), and eluted with a 2.5-L linear gradient of 0–0.5 M NaCl. Gelsolin eluted between 75 and 110 mM NaCl. The protein was dialyzed 24 h versus buffer A, concentrated on DE-52 equilibrated in the same buffer, and eluted stepwise with buffer A + 0.2 M NaCl. The gelsolin was dialyzed versus 2 mM Tris, pH 8.0, and stored at −20 °C. Gelsolin concentration was measured using the bicinchoninic acid method (Smith et al., 1985) using bovine serum albumin as the standard. The functional activity of the gelsolin was assayed by enhancement of the fluorescence of NBD-actin upon gelsolin binding as previously described (Coué & Korn, 1985). NBD-actin was prepared as described previously (Detmers et al., 1981).

Light Scattering. Light scattering was performed as previously described (Fechheimer & Furukawa, 1993). Briefly, mixtures of gelsolin and freshly gel filtered actin were polymerized in 1-cm fluorescence cuvettes with 20 mM Pipes, 1 mM ATP, 50 μM $MgCl_2$, 50 mM KCl, 5 mM EGTA, 0.2 mM dithiothreitol, and 0.02% sodium azide, pH 7.0. The cuvettes, pipette tips, and glassware were rinsed exhaustively with water previously filtered through a 0.22-μm filter in a laminar flow hood to remove dust. All buffers and proteins were filtered through a 0.22-μm filter into dust-free glassware. The protein solutions were mixed in the cuvettes and degassed, salts needed to induce assembly of the actin were added, and then the solutions were immediately mixed by inversion. The cuvettes were then capped and not subjected to any additional shear treatment. The samples were held at room temperature for 24 h before the measurements.

Light scattering measurements were performed at a scattering angle of 90° in a Perkin-Elmer LS-5 spectrofluorometer with polarizing optics. Conventional terminology is that the first letter (capitalized: H or V) indicates the vertical or horizontal plane of polarization of the scattered light, and the second letter (lower case: h or v) indicates the plane of polarization of the incident light. The Vv and Hv components of the scattered light were measured.

Images of Birefringence from Liquid Crystalline Domains. Transmission of polarized light was observed through each sample in which light scattering was measured with dichroic sheet polarizers (catalog no. 47 36 00; Carl Zeiss, Inc., Thornwood, NY) in front of and behind the cuvette. The polarizers were adjusted to extinction with dust-free buffer in a 1-cm cuvette. A 60-W quartz-halogen lamp was utilized as the light source. The light beam passed through a diffuser and a beam expanding lens before illuminating the cuvette. The Vv and Hv components were observed, and images of the Hv transmitted light were recorded on Tri-X film using an Olympus OM-4 camera with a 50-mm macro lens.

Theories Predicting the Formation of Liquid Crystalline Domains. The concentration of actin required to form liquid crystalline domains was calculated employing three different polymer models for the actin filament: uncharged rigid rod, charged rigid rod, and charged worm-like chain. Onsager (1949) predicts that for monodisperse uncharged rigid rods an isotropic to nematic phase transition occurs when the volume fraction of rods exceeds a critical volume fraction of $3.34d/L$ where d and L are the diameter and length of the rod, respectively. Algebraic rearrangement of this expression leads to the result that the transition occurs at $cdL^2 > 4.25$, where c is the concentration of actin in filaments/mL. The diameter of the actin filament was estimated to be 10 nm (Milligan et al., 1990). Number average filament lengths were estimated assuming 1 gelsolin per filament and 364 monomers per micrometer. This assumption has been tested by direct measurement, and the method is quite good in the range of lengths employed in this study, although it must be noted that the distributions are markedly polydisperse (Janmey et al., 1986). The concentration of actin corresponding to the volume fraction at the point of the phase transition was calculated from

$$v_i = cLd^2\pi/4 \quad (1)$$

where v_i is the volume fraction of actin in the isotropic phase, c is the concentration of actin in filaments/mL, and L and d are the length and diameter of a filament, respectively.

The effect of charge on the Onsager model for the phase transition of rigid rods was investigated by Stroobants et al. (1986). They predict that the volume fraction required for the phase transition of charged rigid rods is given by

$$v_i = 3.29 + 2.37/(\kappa d_{eff})$$

where κ is the Debye screening length, and d_{eff} is the effective diameter of a charged rod which includes the effect of hydration and counterion concentration. The effective diameter of the actin filament has been approximated as 12 nm under ionic conditions similar to those employed in our measurements (Matsudaira et al., 1983). The theoretical treatment for charged rods (Stroobants et al., 1986) considers only the presence of monovalent counterions. However, our experimental ionic conditions included polyvalent ions. The equivalent monovalent ion concentration of our solution was estimated by measuring the conductivity and comparing that value to a series of standard KCl solutions. The conductivity of our standard buffer conditions corresponds to a KCl concentration of 87.7 mM. This value was used in estimation of the Debye screening length.

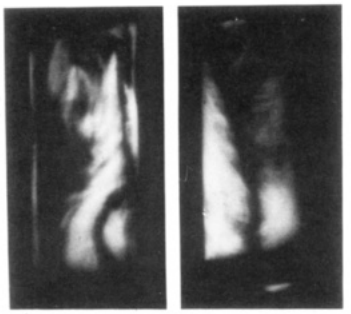

FIGURE 1: Effect of shear on light transmitted through crossed polarizers from a solution containing 2.25 mg/mL actin at a gelsolin: actin ratio of 1/1111 (average filament length 3.0 μm). Samples were either unsheared (A) or sheared by inversion (B). Large randomly oriented domains are apparent in the absence of shear. The sheared sample has a more regular alignment of domains.

The actin filament was also modeled as a charged worm-like chain to determine the effect of the chain flexibility and charge of the actin filament on the formation of liquid crystals (Sato & Teramoto, 1991). This model is a combination of the orientational entropy loss function for worm-like chains (DuPre & Yang, 1991), the excluded volume argument of Onsager extended to charged worm-like chains (Odijk, 1986), and a perturbation calculation of the electrostatic interaction between molecules (Sato & Teramoto, 1991). The phase transition depends on the ratio of the length L to the persistence length ρ, a measure of the chain flexibility, the effective diameter of the chain, and the charge along the chain. Using equations for the osmotic pressure, chemical potential, and molecular distribution parameter α (Inatomi et al., 1992) and minimization routine of multiple variables AMOEBA (Press et al., 1988), the volume fractions of the anisotropic and isotropic phases were calculated. The calculations were performed using an actin persistence length of 12 μm, since this value has been most frequently reported. Since the persistence length of actin has been estimated between 6 and 17.7 μm, some calculations were also performed to determine the effect of varying the persistence length. In this calculation, the effective diameter of the chain is calculated from the diameter of the polymer mass, the surface charge along the polymer, and the ionic conditions. The surface charge density of actin was estimated to be 24 charges per monomer from published titration data (Martonosi et al., 1964). The equivalent KCl concentration was estimated to be 87.7 mM as described above. The actin concentration corresponding to the volume fraction of actin at the phase transition was calculated as described above, but using values for the effective diameter of the filament calculated by the theory.

RESULTS

Evidence for Liquid Crystal Formation by Actin Filaments. Images of light transmitted through crossed polarizers were recorded as an indication of the presence of liquid crystalline domains in unsheared samples of column purified actin assembled in cuvettes. The ordered domains are randomly arranged in unsheared samples as shown by observation of the swirled pattern of birefringence (Figure 1A). The banded pattern is characteristic of nematic liquid crystals. To differentiate liquid crystal formation from the well-characterized effects of shear on alignment of actin filaments monitored as flow birefringence (Cooper & Pollard, 1982), samples that had reached steady state were sheared in a vertical direction by inversion or by pipetting and the polarized transmitted light was examined. After shearing, there is an increase in the amount of birefringence indicating that a further ordering of the actin domains is possible (Figure 1B). The randomly arranged domains were caused to reorient perpendicular to the direction of shear, yielding a brushed pattern.

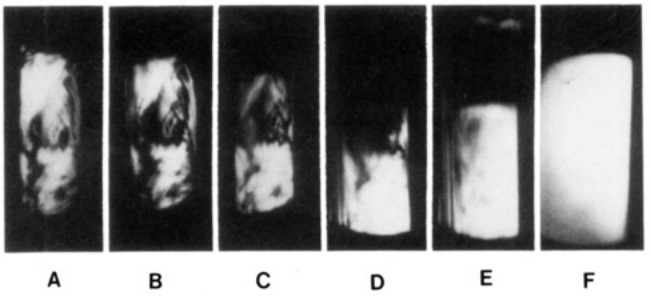

FIGURE 2: Images of polarized light scattered by actin filaments as a function of the angle between the polarizer and analyzer. The light transmitted through 2.25 mg/mL actin at a gelsolin to actin ratio of 1:1111 as a function of the polarization angle of the transmitted light with vertically polarized incident light is shown. (A) 90°; (B) 70°; (C) 60°; (D) 45°; (E) 15°; (F) 0°. The circular edge of the polarizer is seen as a circular edge at the top and/or bottom of the cuvette in some images. Domains are no longer visible when polarizer and analyzer have the same orientation. This result is consistent with formation of liquid crystals and is inconsistent with multiple scattering.

It was possible that the light transmitted through crossed polars was due to multiple scattering. If multiple scattering rather than formation of a liquid crystalline phase was responsible for the swirled pattern, then the observed pattern of the transmitted light would be invariant with polarization. To discriminate between the presence of multiple scattering and birefringence, the polarization of the incident light was held constant and the transmitted light was observed as a function of polarization. The observed transmitted light is shown in Figure 2. The pattern of the transmitted light clearly changes with polarization of the transmitted light and thus must be due to birefringence.

Effects of Actin Concentration and Filament Length on Formation of Liquid Crystals. The formation of oriented arrays and domains in solutions of actin filaments was examined quantitatively using the light scattering technique. The two experimental variables were the concentration of actin and the filament length controlled by varying the ratio of gelsolin to actin at each actin concentration. It is well known that the anisotropic component of the Rayleigh scattering increases dramatically as solutions approach the nematic liquid crystalline phase (Chatelain, 1948; de Gennes, 1974). The Hv/Vv ratio of light scattering intensities was measured as a function of average filament length at an actin concentration of 1.75 mg/mL, a concentration just below the threshold for formation of liquid crystalline domains (see below). At this actin concentration, orientation is maximal at an average length of 4.4 μm corresponding to one gelsolin per approximately 1591 actin monomers and is decreased as the length is varied to longer or shorter values (Figure 3). The reproducibility of the measurement indicated by the precision among identical samples is greatly decreased at longer filament lengths (lower gelsolin to actin ratios).

To study the dependence of liquid crystal formation on average filament length, actin filament concentration was varied at a series of gelsolin to actin ratios between 1:222 (0.6 μm) and 1:1778 (4.9 μm) to vary the average filament length. At an average length of 0.6 μm, the Hv/Vv ratio of light scattering as a function of actin concentration is small and constant (Figure 4A). Liquid crystal formation is not observed at values as high as 3 mg/mL of column purified actin

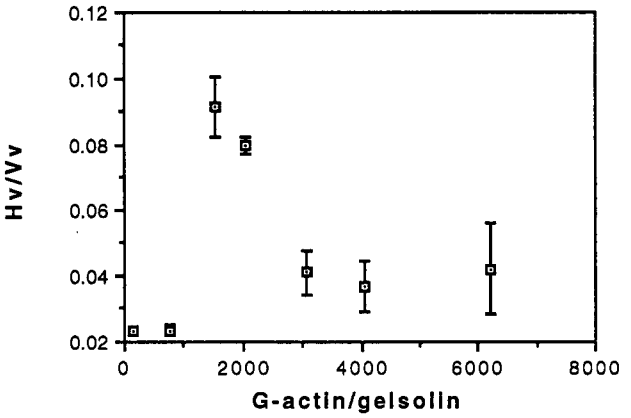

FIGURE 3: Effect of average filament length on orientation at a constant actin concentration. The concentration of actin was maintained at 1.75 mg/ml. The gelsolin to actin ratio was varied as indicated. The Hv/Vv ratio was measured 24 h after mixing. Orientation is optimal at intermediate filament lengths. Note that there is some orientation at this concentration of actin but that the transition to formation of liquid crystal domains is not complete.

assembled into filaments of this length. As the ratio of gelsolin to actin is decreased to increase the average filament length, formation of liquid crystals is observed. The Hv/Vv ratio of light scattering intensity is small at low actin concentrations but increases sharply at higher concentrations of actin (Figure 4B–E). The concentration at which the transition point to higher Hv/Vv light scattering intensity ratios occurs increases moderately with decreasing filament length (Table I).

Macroscopic images of light transmitted through crossed polars were recorded for cuvettes from the experiments in Figure 4. Images of cuvettes containing a gelsolin to actin ratio of 1:1778 (4.9 μm) as a function of actin concentration are shown as a representative example of the complete set of images (Figure 5). At low values of Hv/Vv ratios of the light scattering intensity, the images of the Hv transmitted light are black, indicating that the solution is isotropic. As the concentration of actin increases, swirled patterns become visible in the Hv transmitted light. The observation of these patterns correspond to values of the Hv/Vv ratio of light scattering intensities > 0.1. The increase in the ratio of Hv/Vv light scattering indicates that more of the actin has entered into liquid crystalline domains and/or that the order in the domains increases as the concentration of actin increases.

Comparison of Results to Theoretical Predictions Regarding Liquid Crystal Formation by Actin Filaments. Observations of liquid crystal formation by actin filaments were compared to the models for uncharged rigid rods, charged rigid rods, and charged semiflexible chains (see Materials and Methods). First, the experimental data were transformed, combined, and displayed in a single plot as a function of the cdL^2 parameter, since the models for uncharged rods and charged rods predict that all of the data points will fall on a single curve with a transition at cdL^2 of 4.25 and 3.41, respectively (Figure 6). Our light scattering data form a series of curves which exhibit length dependence. The transition of these curves is observed at values of cdL^2 significantly less than 4.25. The transition value of 3.41 falls among the length dependent curves for our data. Yet, transitions for actin filaments with average lengths of 555 (1.5 μm) and 1111 (3 μm) monomers are significantly below 3.41.

The theoretical models were also employed to predict the volume fraction of actin filaments and thus, the actin concentrations at which formation of nematic domains is expected to occur. The phase transition of 1.5 and 3.0 μm

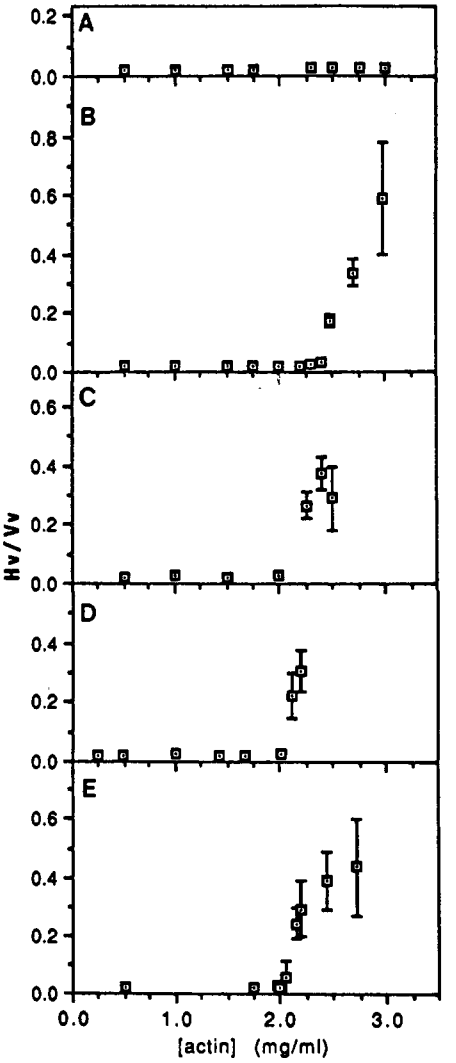

FIGURE 4: Ratio of Hv/Vv scattered light intensities as a function of average actin filament length and actin concentration. (A) 1:222 gelsolin:actin ratio (0.6 μm); (B) 1:555 gelsolin:actin ratio (1.5 μm); (C) 1:1111 gelsolin:actin ratio (3.0 μm); (D) 1:1591 gelsolin:actin ratio (4.4 μm); (E) 1:1778 gelsolin:actin ratio (4.9 μm). The concentration of column purified actin was varied from 0.5 to as high as 3 mg/mL as indicated in the figure. The mean value and standard deviation are calculated from at least three points. Data points for which the error bars are not visible in the figure have standard deviations that are not larger than the symbol.

Table I: Actin Concentration Required for Liquid Crystal Formation as a Function of Average Filament Length

actin:gelsolin	length (μm)	concentration (mg/mL)
222	0.6	>3.00
555	1.5	2.40
1111	3.0	2.12
1591	4.4	2.07
1778	4.9	2.03

chains occurred at actin concentrations much lower than that predicted by the Onsager model (Figure 7, curve 2), while the longer chains were predicted correctly. The effect of electrostatic charge on a rigid rod is to lower the concentrations predicted by Onsager by approximately 20% (Figure 7, curve 3). This predicts that, at average lengths greater than 4 μm, the phase transition to a nematic phase should have occurred at lower concentrations than were observed. The actin concentration predicted for the shorter chains of 1.5 and 3.0 μm was greater than that observed. The values of the volume fractions of actin filaments required to achieve a phase

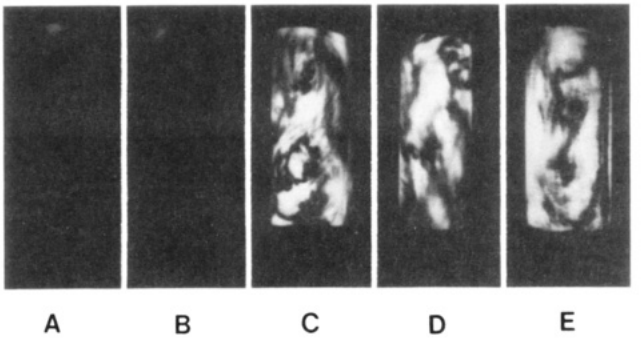

FIGURE 5: Polarized transmitted light images of actin solutions at fixed length and increasing concentration. The gelsolin to actin ratio was held at 1778 (average filament length of 4.9 μm). The actin concentrations were: (A) 1.75 mg/mL; (B) 2.05 mg/mL; (C) 2.15 mg/mL; (D) 2.2 mg/mL; (E) 2.48 mg/mL. These images were recorded from the same cuvettes reported in Figure 4E.

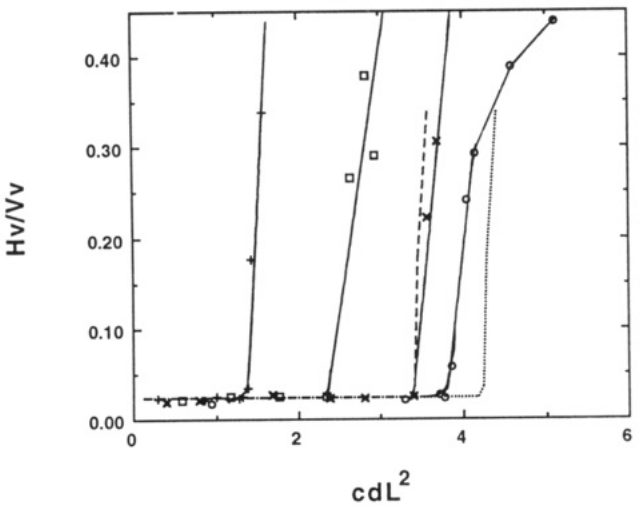

FIGURE 6: Actin forms oriented domains at lower concentrations than predicted by the theories for uncharged and charged rods. The ratio of the Hv/Vv scattered light intensities is shown as a function of the actin concentration (c), diameter (d), and length squared (L^2). Calculations of cdL^2 for our data were made using a diameter of 10 nm for the actin filament and assuming 364 actin monomers/micrometer of filament. Data values obtained from actin filament lengths of 222 (0.6 μm, △), 555 (1.5 μm, +), 1111 (3.0 μm, □), 1591 (4.4 μm, ×), and 1778 (4.9 μm, ○) monomers per filament are shown. A family of curves representing the length distributions employed is observed. The models for uncharged and charged rigid rods predict a single curve that fits the data for all lengths that makes a transition at $cdL^2 > 4.25$ and 3.41, respectively. Theoretical curves corresponding to the models for uncharged (···) and charged (- - -) rods are shown.

transition required by the theory for charged persistent chains (Sato & Teramoto, 1991) (Figure 7, curve 1) are greater than that predicted by the theories for uncharged and charged rods, and the actin concentrations at which phase transitions are predicted to occur are correspondingly greater. The predicted values of the phase transition for charged worm-like chains are larger than those experimentally observed (Table I). For all models considered, the volume fraction required for a phase transition is markedly length dependent. This is in contrast to the moderate length dependence of the observed values.

DISCUSSION

Empirical Observations on Liquid Crystal Formation by Actin. Formation of oriented domains in actin solutions was observed previously in studies of the rheology of actin solutions at concentrations of 6–25 mg/mL actin (Buxbaum et al., 1987; Kerst et al., 1990). The rheological behavior was interpreted as flow and orientation of nematic domains under shear.

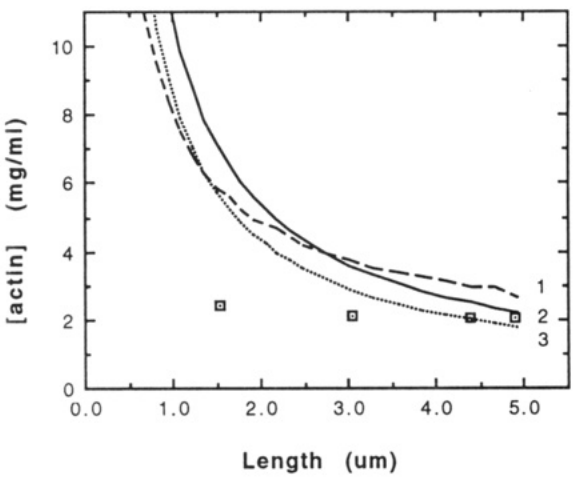

FIGURE 7: Comparison of experimentally observed values of the liquid crystalline phase transition versus theoretically predicted values. The experimentally observed values (□) of the phase transition are shown as a function of length. The theoretical predictions of the models for charged worm-like chains (curve 1, - - -), uncharged rods (curve 2, —), and charged rods (curve 3, ···) are shown for comparison. The predicted length dependence of all three of the models is greater than that observed for actin. All of the models deviate most significantly from the data at the shorter average filament lengths.

Formation of aligned domains in solutions of pure actin at 1 mg/mL induced by controlled linear shear has been recently documented in an elegant combined optical/rheological study (Cortese & Frieden, 1988). Suzuki and colleagues (1991) and Coppin and Leavis (1992) have previously reported that formation of a liquid crystalline phase in solutions of filamentous actin depends on the average length distribution of the actin filaments. These studies reported actin concentration values at which the phase transitions were observed that are consistently 2–4-fold higher than those reported in this study, especially for shorter filaments. These differences are attributable to the fact that the average filament lengths actually present in the prior studies are likely to be shorter than were reported. Methods used for preparation of actin in the previous studies indicate the presence of significant quantities of endogeneous capping protein and/or actin oligomers that could add nuclei to the solutions, thereby increasing the number concentration of filaments and decreasing the average length. In addition, the filaments in one of the previous studies were "gently agitated by a couple of upside-down inversions" to accelerate formation of the liquid crystalline phase (Suzuki et al., 1991). It seems likely that shearing of the filaments may have further decreased the average length, thereby increasing the concentration required for the phase transition, or caused the formation of the nematic phase by shear induced alignment.

Comparison of Empirical Observations to Theories Predicting the Formation of Liquid Crystalline Domains. The data for formation of liquid crystals in solutions of actin filaments have been compared to predictions of the models for uncharged rigid rods (Onsager, 1949), for charged rigid rods (Stroobants et al., 1986), and for charged worm-like chains (Sato & Teramoto, 1991). All three models are based on the assumption that the polymers have a monodisperse length distribution. All three models predict a greater length dependence of the concentration required for the phase transition than is experimentally observed. The contributions of charge and hydration have been estimated by modeling (Figure 7) and do not appear sufficient to explain the discrepancies of our data to the liquid crystal theory. Rather, these deviations may be due to uncertainty in the persistence

length and/or length polydispersity of the actin filaments.

To evaluate the effect of the persistence length on predictions of the model for charged worm-like chains, we have varied the value of the persistence length used in the calculation. If the persistence length decreases from 12 to 6 μm, the values of the predicted phase transition increases by approximately 30%. If the value of the persistence length increases to 17 μm, the values of predicted phase transition decreases by approximately 15%. In the most favorable case, that is the persistence length is 17 μm, the predicted values of the phase transition are still significantly greater than the observed values at all lengths. There is one report (Schmidt et al., 1989) that suggests that actin filaments can be modeled as flexible chains, i.e., the persistence length is very small. The value of the predicted concentration required for a phase transition increases with decreasing values of the persistence length, increasing the discrepancy between our experimental data and the theoretically predicted phase transition. Thus, no single value of the persistence length can reconcile the predictions of the models with our data over the full range of average filament lengths.

A more likely explanation of the disagreement between the predicted and observed concentrations at which liquid crystal formation is observed is that the filament lengths are not constant but rather are polydisperse forming an exponential distribution (Janmey et al., 1986; Kawamura & Maruyama, 1970). The longest filaments influence the concentration required for a phase transition for rod-like chains with polydisperse length distributions (Flory & Abe, 1978; Lekkerkerker et al., 1984). Comparison between monodisperse and polydisperse filament populations having equal number average filament lengths reveals that, in polydisperse systems, the longest filaments are predicted to preferentially enter the nematic phase and lower the concentration required for the transition below that of a monodisperse solution of filaments. This has been experimentally observed for mixtures of different molecular weight samples of schizophyllan, a charged worm-like chain polysaccharide (Itou & Teramoto, 1984; Van & Teramoto, 1984). This effect could contribute to the fact that the observed transitions to formation of the liquid crystalline phase is at a lower concentration of actin than predicted by the models. In addition, length polydispersity is the most likely explanation for the fact that the observed effects of changes in filament length on the concentration required for the transition is much less than is predicted by the models. The effect of polydispersity on the phase transition of actin was not calculated due to the lack of tractable theoretical equations.

Our measurements performed using a fixed concentration of actin below that required for the transition to the nematic phase indicate that orientation was optimal at intermediate average filament lengths (Figure 3). This could be due to kinetic constraints imposed by the slower rotational and translational diffusion of long filaments and entanglements which impede the spatial rearrangement of the filaments. In addition, the higher observed value of Hv/Vv could be due to increased orientational correlation among the filaments in the aligned domains at intermediate filament lengths, since longer filaments show greater deviation from a rod. Indeed, maximal orientation among filaments of intermediate lengths has been predicted for worm-like chains (DuPre & Yang, 1991).

Biological Significance of Formation of Liquid Crystalline Domains by Actin. The observation that liquid crystals form in actin solutions at concentrations lower than previously reported demonstrates the potential physiological significance of this phenomenon. That is, liquid crystals could form in cells. The average filamentous actin content of a typical eucaryotic cell is 5 mg/mL assuming 10% of cell protein is actin and 50% of the actin is in polymeric form. Cellular extensions such as microvillar core bundles may have actin filament concentrations as high as 150 mg/mL (Matsudaira et al., 1983). It has been estimated that 96% of the filamentous actin in *Dictyostelium* is present in filaments 0.22 μm in length, 3% in filaments 1.3 μm in length, and 0.3% in filaments 13 μm in length (Podolski & Steck, 1990). The theory of Onsager predicts that actin filaments 0.22 μm long would form liquid crystals at a concentration of 30 mg/mL. Using the difference between the predictions of the theory and our *in vitro* data of approximately 4-fold at a length of 1.5 μm, the filaments could form liquid crystals at concentrations of 7.5 mg/mL in cells, well within the physiological range. The presence of approximately 100 mg/mL of protein in cytosol occupies a large volume fraction in the milieu of the actin filaments *in vivo*. Occupancy of a large fraction of the volume could further contribute to formation of the liquid crystalline phase. The theoretical case of mixtures of rod-like particles with random coils has been considered by Flory (1978). The addition of random coils drives the formation of the ordered phase and also causes the rod-like particles to segregate in the nematic phase with almost total exclusion of the coils from this phase. In support of the latter suggestion, it has been shown that gentle shear coupled with addition of high concentrations of poly(ethylene glycol) or ovalbumin induces formation of filament bundles in solutions containing only 0.5 mg/mL polymerized actin (Suzuki et al., 1989).

The formation of liquid crystals could profoundly affect the rheological properties of cytoplasm or of actin *in vitro*. The flow of domains model for the rheology of cytoplasm and of liquid crystals of actin has been discussed previously (Buxbaum et al., 1987; Kerst et al., 1990). While the formation of local arrays of oriented actin filaments could promote formation of cellular extensions and the bundling of actin by actin bundling proteins, it cannot account for the polarity of the filaments within these domains. Establishment of a local region with high alignment among actin filaments could correspond to the nucleation step recently proposed to initiate the process of actin filament bundle formation by sea urchin fascin (Stokes & DeRosier, 1991). The establishment of conditions for formation of liquid crystalline domains with pure actin in the absence of shear allows direct test of the hypothesis that self-orientation of actin filaments promotes formation of actin filament bundling. Understanding the basic mechanisms directing the formation of oriented and cross-linked actin structures will lead to new insights regarding dynamic changes in cytoplasmic structure accompanying cell movements. Spontaneous ordering, osmotic effects, shear, and actin binding proteins can all contribute to formation of ordered actin structures. Assessing the relative contributions of these factors in determination of cell shape and cytoplasmic structures is a significant challenge for future research.

ACKNOWLEDGMENT

We thank the laboratory of Dr. M. J. Cormier (Department of Biochemistry, University of Georgia) for the use of the spectrofluorometer and polarization optics.

REFERENCES

Burlacu, S., Janmey, P. A., & Borejdo, J. (1992) *Am. J. Physiol. 262*, C569–C577.

Buxbaum, R. E., Dennerll, T., Weiss, S., & Heidemann, S. R. (1987) *Science 235*, 1511–1514.

Chatelain, P. (1948) *Acta Crystallogr. 1*, 315.
Cooper, J. A., & Pollard, T. D. (1982) *Methods Enzymol. 85*, 182–210.
Cooper, J. A., Bryan, J., Schwab, B., Frieden, C., & Loftus, D. J. (1987) *J. Cell Biol. 104*, 491–501.
Coppin, C. M., & Leavis, P. C. (1992) *Biophys. J. 63*, 794–807.
Cortese, J. D., & Frieden, C. (1988) *J. Cell Biol. 107*, 1477–1487.
Coué, M., & Korn, E. D. (1985) *J. Biol. Chem. 260*, 15033–15041.
de Gennes, P.-G. (1974) *The Physics of Liquid Crystals*, Clarendon Press, Oxford.
Detmers, P., Weber, A., Elzinga, M., & Stephens, R. E. (1981) *J. Biol. Chem. 256*, 99–105.
DuPre, D. B., & Yang, S. (1991) *J. Chem. Phys. 94*, 7466–7477.
Fechheimer, M., & Furukawa, R. (1993) *J. Cell Biol. 120*, 1169–1176.
Flory, P. J. (1978) *Macromolecules 11*, 1138–1141.
Flory, P. J., & Abe, A. (1978) *Macromolecules 11*, 1119–1122.
Furukawa, R., Kundra, R., & Fechheimer, M. (1992) *Mol. Biol. Cell. 3*, 38a.
Gittes, F., Mickey, B., Nettleton, J., & Howard, J. (1993) *J. Cell Biol. 120*, 923–934.
Hitt, A. L., Cross, A. R., & Williams, R. C. J. (1990) *J. Biol. Chem. 265*, 1639–1647.
Inatomi, S., Jinbo, Y., Sato, T., & Teramoto, A. (1992) *Macromolecules 25*, 5013–5019.
Itou, T., & Teramoto, A. (1984) *Macromolecules 17*, 1419–1420.
Janmey, P. A., Peeterman, J., Zaner, K. S., Stossel, T. P., & Tanaka, T. (1986) *J. Biol. Chem. 261*, 8357–8362.
Kawamura, M., & Maruyama, K. (1970) *J. Biochem. (Tokyo) 67*, 437–457.
Kerst, A., Chmielewski, C., Livesay, C., Buxbaum, R. E., & Heidemann, S. R. (1990) *Proc. Natl. Acad. Sci. U.S.A. 87*, 4241–4245.
Lekkerkerker, H. N. W., Coulon, P., Van der Haegen, R., & Devlieck, R. (1984) *J. Chem. Phys. 80*, 3427–3433.
MacLean-Fletcher, S. D., & Pollard, T. D. (1980) *Biochem. Biophys. Res. Commun. 96*, 18–27.
Martonosi, A., Molino, C. M., & Gergely, J. (1964) *J. Biol. Chem. 239*,
Matsudaira, P., Mandelkow, E., Renner, W., Hesterberg, L. K., & Weber, K. (1983) *Nature 301*, 209–214.
Milligan, R. A., Whittaker, M., & Safer, D. (1990) *Nature 348*, 217–221.
Nagashima, H., & Asakura, S. (1980) *J. Mol. Biol. 136*, 169–182.
Odijk, T. (1986) *Macromolecules 19*, 2313–2329.
Onsager, L. (1949) *Ann. N.Y. Acad. Sci. 51*, 627–659.
Oosawa, F. (1980) *Biophys. Chem. 11*, 443–446.
Podolski, J. L., & Steck, T. L. (1990) *J. Biol. Chem. 265*, 1312–1318.
Press, W. H., Flannery, B. P., Teukolsky, S. A., & Vetterling, W. T. (1988) *Numerical Recipes in C. The Art of Scientific Computing*, Cambridge University Press, Cambridge.
Sato, T., & Teramoto, A. (1991) *Physica A 94*, 72–86.
Schmidt, C. F., Bärmann, M., Isenberg, G., & Sackmann, E. (1989) *Macromolecules 22*, 3638–3649.
Smith, P. K., Krohn, R. I., Hermanson, G. T., Mallia, A. K., Gartner, F. H., Provenzano, M. D., Fujimoto, E. K., Goeke, N. M., Olson, B. J., & Klenk, D. C. (1985) *Anal. Biochem. 150*, 76–85.
Spudich, J. A., & Watt, S. (1971) *J. Biol. Chem. 246*, 4866–4871.
Stokes, D. L., & DeRosier, D. J. (1991) *Biophys. J. 59*, 456–465.
Stroobants, A., Lekkerkerker, H. N. W., & Odijk, T. (1986) *Macromolecules 19*, 2232–2245.
Suzuki, A., Yamazaki, M., & Ito, T. (1989) *Biochemistry 28*, 6513–6518.
Suzuki, A., Maeda, T., & Tadanao, I. (1991) *Biophys. J. 59*, 25–30.
Van, K., & Teramoto, A. (1984) *Polym. J. (Tokyo) 17*, 409.
Yanagida, T., Nakase, T., Nishiyama, K., & Oosawa, F. (1984) *Nature 307*, 58–60.